

Standing spin wave mode in RFIM at $T=0$: Patterns and athermal nonequilibrium phases

Muktish Acharyya

*Department of Physics, Presidency University,
86/1 College street, Calcutta-700073, INDIA.
E-mail:muktish.physics@presiuniv.ac.in*

Abstract: The dynamical responses of random field Ising model at zero temperature, driven by standing magnetic field wave, is studied by Monte Carlo simulation in two dimensions. The three different kinds of distribution of quenched random field are used here, uniform, bimodal and Gaussian. In all cases, three distinct dynamical phases were observed, namely, the *pinned*, *structured* and *random*. In the pinned phase no spin flip is observed. In the structured phase standing spin wave modes are observed. The random phase is shown with no observed regular pattern. For a fixed value of the amplitude of the standing magnetic field wave, in the region of small quenched field, the system remains in a pinned phase. In the intermediate range of values of random field, a standing spin wave mode (structured phase) is observed. The regular pattern of this spin wave mode disappears for higher values of random field yielding a random phase. The comprehensive phase boundaries are drawn in all three cases. The boundary of pinned phase are analytically calculated for uniform and bimodal types of quenched random fields.

Keywords: RFIM, Standing wave, Quenched random field, Monte Carlo simulation

1. Introduction:

The random field Ising model (RFIM) is a simple model to understand various physical phenomena, like, hysteresis[1], Barkhausen noise [2] observed in ferromagnetic materials, avalanche[3], return point memory effects etc. The RFIM was studied theoretically with intense attention. RFIM was solved exactly[4] on Bethe lattice and the qualitative behaviour of magnetisation as a function of external magnetic field was found to depend on the coordination number of Bethe lattice. The effect of coordination number on the nonequilibrium critical point in RFIM was studied[5] in details. Hysteresis in RFIM with asymmetric distribution of quenched random fields in the limit of low disorder was studied[6] and the spin flip was found to be related to bootstrap percolation. Athermal hysteresis was also studied[7] in antiferromagnetic RFIM recently. The statistics[8] and the dynamical critical behaviour of avalanches[9] was studied in RFIM. All these studies mentioned here are static in a sense that the time dependence of any quantity is studied.

The dynamical behaviours of the driven RFIM are also quite interesting. The RFIM has also served to study the dynamics of domain wall. The motion of domain wall by magnetic field in a 2D ultrathin Pt/Co/Pt film (showing perpendicular anisotropy and quenched disorder which is analogous to RFIM) was studied[10] experimentally by magneto optical polar Kerr imaging technique. The motion of moving interface was analyzed numerically[11] in the RFIM driven by external magnetic field. Later, the depinning transition of driven interface was studied[12]. The creep motion of interface in driven RFIM was studied [13] and the nonlinear field-velocity relationship was found.

All the studies mentioned above have a very common feature. Firstly, the external driving magnetic field was varied in a quasi-static manner. Secondly, the driving magnetic field is uniform over the lattice at any given instant of time. The RFIM also shows interesting dynamical behaviours if the uniform driving field varies rapidly. The dynamic hysteresis and dynamical athermal phase transition was already studied[14] in RFIM. More interesting news comes from the fact when RFIM is driven by a field having both spatio-temporal variation. Very recently, the RFIM was studied[15] in the presence of propagating magnetic field wave. Various nonequilibrium phases are observed[15] and a phase boundary was drawn. In this paper, the dynamical responses of RFIM driven by standing magnetic field wave is studied in details. The paper is organised as follows: the model and simulation are discussed in section-2, numerical results are reported in section-3 and the paper ends with a summary of the work in section-4.

2. Model and simulation:

The Ising model on a square lattice ($L \times L$), in the presence of quenched random magnetic field and driven by a magnetic field having spatio-temporal variation, can

be described by the Hamiltonian,

$$H = -J \sum s(x, y, t) s(x', y', t) - \sum h_r(x, y) s(x, y, t) - \sum h_s(x, y, t) s(x, y, t). \quad (1)$$

Where $s(x, y, t) = \pm 1$ is Ising spin at site (x,y) and at time t . $J > 0$ is ferromagnetic spin-spin interaction (nearest neighbour only) strength, $h_r(x, y)$ is quenched random field and $h_s(x, y, t)$ is external magnetic field having spatio-temporal variation. In the present study, $h_s(x, y, t)$ represent the value of the external magnetic field at lattice site (x,y) and at time t . The standing magnetic wave field $h_s(x, y, t)$ can be represented as

$$h_s(x, y, t) = h_0 \sin(2\pi f t) \sin\left(\frac{n\pi y}{L}\right). \quad (2)$$

Where, h_0 and f represent the amplitude and frequency of the standing magnetic field wave respectively. Here, n represents the number of antinodes in the standing magnetic wave. The standing magnetic field wave spreads along the y direction only. The periodic boundary conditions are applied in both directions.

The distributions of the quenched random field $h_r(x, y)$, are considered here of following three types:

(a) The uniformly distributed between $-w$ and $+w$, with probability $P_u(h_r) = \frac{1}{2w}$ if $-w \leq h_r \leq +w$ and 0 otherwise.

(b) Having a bimodal probability distribution

$$P_b(h_r) = 0.5\delta(h_r - w) + 0.5\delta(h_r + w). \quad (3)$$

where δ represents the Dirac delta function.

(c) The normally distributed with 0 mean and standard deviation σ ($=2w$ here) with probability

$$P_n(h_r) = \frac{1}{\sqrt{2\pi\sigma^2}} e^{-\frac{h_r^2}{2\sigma^2}} \quad (4)$$

This RFIM driven by standing magnetic field wave is studied by Monte Carlo simulation at zero temperature. The zero temperature Metropolis dynamics is considered here in the manner that the spin only flips if it lowers the energy[16]. Starting from an initial configuration as

$$s(x, y, t = 0) = +1 \quad \forall \quad x, y. \quad (5)$$

The parallel updating rule is used here. L^2 such updates of spins constitutes the unit time step, i.e. Monte Carlo Step (MCS). Throughout the simulation the frequency of the standing magnetic field wave is kept constant ($f = 0.01$). So, time period $\tau = 100$ MCS is required to have a complete temporal cycle of the standing magnetic field wave. For n loop standing wave, one would get n number of antinodes in the length L . As a result the wavelength of the standing magnetic field wave $\lambda = 2L/n$. Here, the simulation is done and the results are shown for $n = 4$ and $n = 2$. The linear size of the square lattice is chosen $L = 100$ here. The wavevector, $k = \frac{2\pi}{\lambda}$.

3. Numerical Results:

Here, the dynamical responses of the model are studied for three different kinds of the distributions of quenched random field. For uniformly distributed (eqn-3) quenched random field, depending on the values of w , h_0 mainly three different kinds of dynamical or nonequilibrium phases are observed. For $h_0 = 1.0$ and $w = 1.0$, the RFIM remains pinned, i.e., no spin flips was observed. This is called *pinned* phase. For the higher values of h_0 and w , namely $h_0 = 2.0$ and $w = 3.0$, a *structured* phase was observed. Here, the band like sturcture of the clusters of the spins are formed. These bands oscillates periodically as the fields changes sign in the standing magnetic field wave. A typical phase of this kind may be found in a video presentation in <http://youtu.be/5pzW3chzYnw>. Note that the value of the n is taken here equals to 4. That corresponds to the presence of 4 antinodes in the standing magnetic field wave. For $h_0 = 1.0$ and $w = 5.0$, a random spin configuration (with no specific structure) is found. This is called *random* phase. Figure-1 shows snapshots of such dynamical phases.

For a particular value of h_0 , the three phases (mentioned above) are found by varying the strength of the quenched random field w . The system remains in a pinned phase untill a value of w is reached. After that, it remains in the structured phase and ultimately it reaches the random phase for much higher values of w .

All these nonequilibrium phases can be characterise by the following quatitites: the dynamic structure factor $S(k, t) = (1/L) \int_0^L m(y, t) e^{iky} dy$, where the line magnetisation along y direction is defined as $m(y, t) = (1/L) \int_0^L s(x, y, t) dx$. Here, the integrals are essentially the summation over discrete lattice point. The time average magnetisation over the full cycle of the standing magnetic field wave is defined as $Q = \frac{1}{L\tau} \oint m(y, t) dt$. Here also, the integral is essentially the discrete sum over the MCS. All these quantities are obtained by averaging over 100 different samples of quenched random field.

In the pinned phase, the structure factor $S(k, t)$ will be zero and Q will be unity. However, in the structured phase $S(k, t)$ is nonzero and Q will be less than unity (due to the presence of spins of opposite sign). In the random phase, where no specific pattern is present and approximately 50 per cent of the total number of spins have opposite sign. As a result, Q and $S(k, t)$ will be nearly equal to zero. For a fixed value of h_0 the transition from pinned to random via the structured phase was observed by studying the $S(k, t)$ and Q as functions of w . In the case of uniformly distributed quenched random field, Figure-2 shows such variations for $h_0 = 2.0$ and $h_0 = 3.0$. Here, the n is chosen equal to 4. For small values of w , the system remains in pinned phase ($|S(k, y)| = 0.0$ and $Q = 1.0$ in fig.2(a) and fig.2(b)). Above a particular value of w , the system transits to the structured (middle of Fig-1) phase, where $|S(k, t)|$ shows a large nonzero value and Q becomes less than unity. This transition point can be marked by a sharp maximum and minimum of the derivatives $\frac{d(|S(k, t)|)}{dw}$ and $\frac{dQ}{dw}$ respectively (fig.2(c) and fig.2(d)). This transition point is w_p . As the w increases, both Q and $|S(k, t)|$ decreases and eventually vanishes in the random phase. It is observed that structured phase persists as long as $|S(k, t)|$

remains larger than 0.1. The structure completely disappears for $|S(k, t)| < 0.1$ and the system gets into random phase. The transition from structured to random phases are marked by $|S(k, t)| < 0.1$. This transition point is called w_s . It is noted that, the transition values of the quenched random field, w_p and w_s depend on the value of h_0 . The w_p decreases as h_0 increases. Physically, larger amount of standing wave field is required to flip the spin for weak quenched random field. On the other hand, w_s increases as w increases upto a certain value of w .

The comprehensive phase boundaries (pinned-structured and structured-random) can be plotted in the plane described by h_0 and w . It is shown in fig-3. It may be noted the the bounadry of pinned and structured phases is linear. This can be realised as follows: the spin flip will not be possible until the local field is negative. The local field $F = 4 - (w + h_0)$ remains positive as long as $w + h_0 < 4$, preventing the spin flip. So, the boundary of pinned phase is nothing but a straight line $w + h_0 = 4$. The phase boundaries are also obtained for $n = 2$. No considerable difference was observed.

The similar studies were done for bimodal distribution (eqn-4) of quenched random field. The qualitative behaviours are similar to that observed in the case of uniformly distributed quenched random field. Figure-4 shows the plots of $|S(k, t)|$, Q and the derivatives $\frac{d(|S(k, t)|)}{dw}$ and $\frac{dQ}{dw}$ as functions of w for two different values of h_0 . The comprehensive phase boundaries (for $n = 4$ and $n = 2$) are shown in figure-5. Here, the boundary of pinned-structured phase is linear and same argument may be applied to analyse it. However, the boundary of structured-random phase for higher values of h_0 is a line $w = 4.0$. As the distribution is bimodal, w can be +4 or -4. So, for larger values of h_0 , $w = 4.0$ will randomise the spin structure.

The normally distributed (eqn-5) quenched random field was also used to study the dynamical or nonequilibrium behaviour of RFIM at $T = 0$. Here also, qualitatively similar kind of behaviours were observed. Figure-6 shows the plots of $|S(k, t)|$, Q and the derivatives $\frac{d(|S(k, t)|)}{dw}$ and $\frac{dQ}{dw}$ as functions of w for two different values of h_0 . However, the region of pinned phase is much smaller than that for other two (uniform and bimodal) cases. The quality of the data is not quite conclusive to get any analytic form of the phase boundary. The comprehensive phase boundaries (for $n = 4$ and $n = 2$) are shown in figure-7.

4. Summary:

The nonequilibrium behaviours of the random field Ising ferromagnet, at zero temperature, driven by standing magnetic field wave are studied by Monte Carlo simulation in two dimensions. The three different kinds, namely, uniform, bimodal and Gaussain, of distributions of the quenched random fields are considered here. The random field Ising ferromagnet is driven by an additional standing magnetic field wave of well defined amplitude, frequency and wavelength. The wavelength depends

on the number of antinodes are present in the standing wave. In the present study, only 2-loop and 4-loop standing waves are considered. Starting from an initial spin configuration having all spins are up, the zero temperature Metropolis dynamics are employed. In this case, the spin only flips if its lowers the energy. The rule parallel updating is used here.

In the dynamical steady state, the system shows three distinct nonequilibrium phases depending on the values of the amplitude of standing magnetic field wave and the strength of quenched random field. For a fixed value of the amplitude of the standing magnetic field wave, in the limit of weak quenched random field, the system remains in a pinned phase. In this phase, all spins remain up as considered in the initial configuration. In the intermediate values of the quenched random field, a standing spin wave mode is observed. Here, the bands of up and down spins formed alternately and oscillates. This is different from the propagation mode studied[15] earlier in RFIM driven by propagating magnetic field wave. Where the bands of alternate up and down spins moved in the direction of the propagating magnetic field wave.

The comprehensive phase boundaries are drawn in the plane formed by the strength of random field and the amplitude of standing magnetic field wave. These phase boundaries are qualitatively similar in three different kinds of distributions of quenched random field. The boundaries of pinned phases in the cases of uniform and bimodal distribution can be obtained analytically.

The compound $\text{LiHo}_x\text{Y}_{1-x}\text{F}_4$ can be modelled by random field Ising model. On applying standing magnetic field wave, a possible way to see these effects experimentally, may be the relaxation experiments using SQUID magnetometer [17].

Acknowledgements: Author would also like to thank Ritaban Chatterjee for his help to prepare the video of standing spin wave modes.

References

1. *The science of hysteresis*, Eds. G. Bertotti and I. Mayergoyz, Academic Press, Amsterdam (2006); See also, T. Nattermann in *Spinglasses and Random Fields*, Ed. A. P. Young, World Scientific, Singapore (1997).
2. J. P. Sethna, K. Dahmen, S. Kartha, J. A. Krumhansl, B. W. Roberts and J. D. Shore, *Phys. Rev. Lett.* **70** (1993) 3347
3. O. Perkovic and K. Dahmen, *Phys. Rev. Lett.* **75** (1995) 4528

4. D. Dhar, P. Shukla and J. P. Sethna, *J. Phys: Math. Gen.* **30** 5259
5. D. Thongjamayum and P. Shukla, *Phys. Rev. E* **88** (2013) 042138
6. S. Sabhapandit, D. Dhar and P. Shukla, *Phys. Rev. Lett.* **88** (2002) 197202
7. L. Kurbah and P. Shukla, *Phys. Rev. E* **83** (2011) 061136
8. B. Tadic, *Physica A* **270** (1999) 125
9. B. Tadic and U. Nowak, *Phys. Rev. E* **61** (2000) 4610
10. S. Lemerele, J. Ferre, C. Chappert, V. Mathet, T. Giamarchi and P. L. Doussal, *Phys. Rev. Lett.* **80** (1998) 849
11. L. Roters, U. Nowak and K. D. Usadel, *Phys. Rev. E* **63** (2001) 026113
12. L. Roters, S. Lubeck and K. D. Usadel, *Phys. Rev. E* **66** (2002) 026127
13. R. H. Dong, B. Zhang and N. J. Zhau, *Eur. Phys. Lett.* **98** (2012) 36002; See also, U. Nowak and K. D. Usadel, *Eur. Phys. Lett.* **44** (1998) 634
14. M. Acharyya, *Physica A* **252** (1998) 151
15. M. Acharyya, *J. Magn. Magn. Mater.* **334** (2013) 11
16. R. J. Glauber, *J. Math. Phys.* **4** (1963) 294
17. L. Thomas and B. Barbara, *J. Low. Temp. Phys.* **113** (1998) 1055

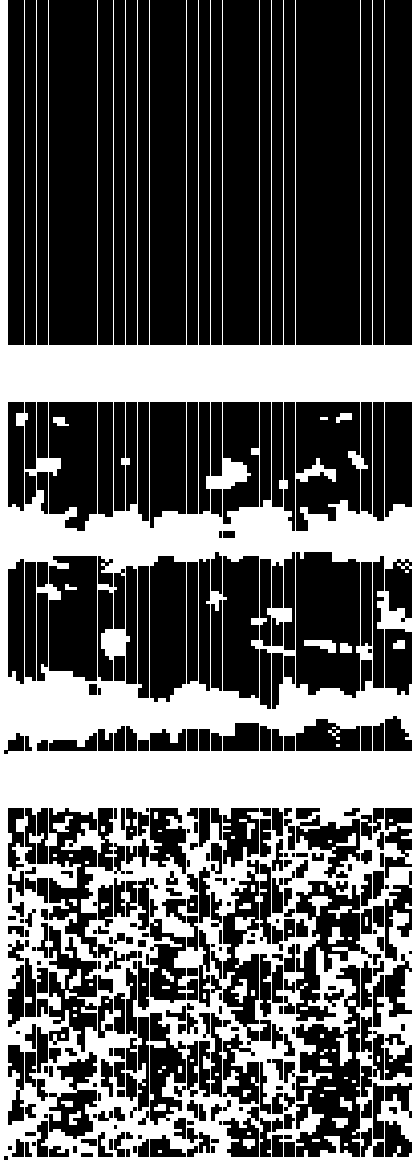


Fig-1. The snapshots (taken after $t = 100$ MCS) of spin configuration for uniform distribution of quenched random field. The black dots represent $s(x, y, t) = +1$. The pinned phase is shown (for $h_0 = 1.0$, $w = 1.0$) in the top. The structured (for $h_0 = 2.0$, $w = 3.0$) phase is shown in the middle. The bottom one shows the random (for $h_0 = 1.0$, $w = 5.0$) phase. Here, $L = 100$ and 4-loop standing magnetic field wave is considered in each case. The dynamics of the structured phase can be found in <http://youtu.be/5pzW3chzYnw>.

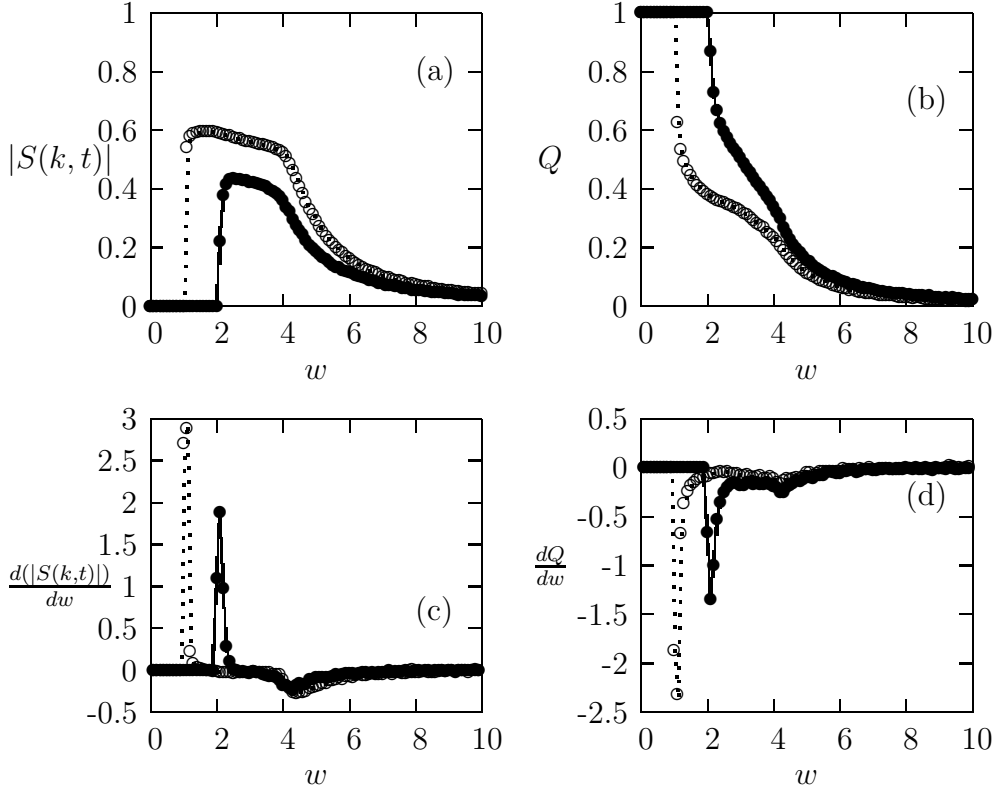


Fig-2. The $|S(k, t)|$, Q , $\frac{d(|S(k, t)|)}{dw}$ and $\frac{dQ}{dw}$ are plotted against w for uniform distribution of quenched random field for two different values of h_0 and 4-loop of standing magnetic field wave. Different symbols represent different values of h_0 . (\bullet) represents $h_0 = 2.0$ and (\circ) represents $h_0 = 3.0$. Solid and dotted lines are just connecting the data points.

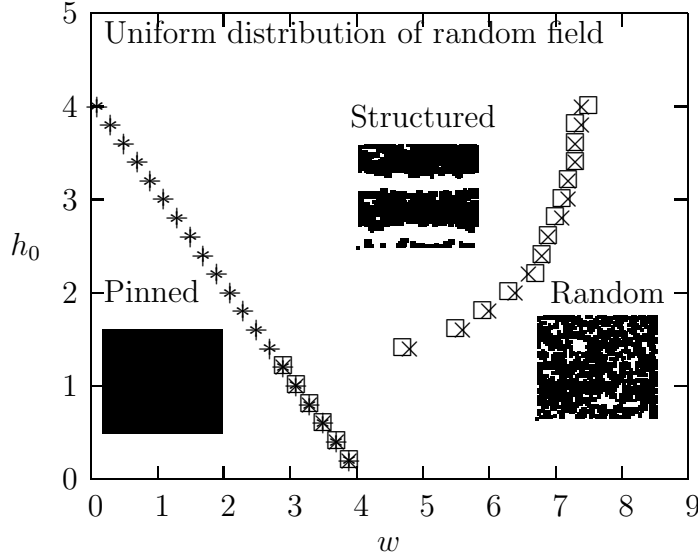


Fig-3. The phase diagram for uniform distribution of quenched random field. The boundaries of pinned-structured (+) phase and the structured-random (\times) phase are shown for $n = 2$. The boundaries of pinned-structured (*) phases and the structured-random (\square) phases are also shown for $n = 4$. The typical spin configurations (for 60×60 lattice) are shown in the insets for three different phases. The pinned phase ($h_0 = 1.0, w = 1.0$), the structured phase ($h_0 = 2.0, w = 3.0$) and the random phase ($h_0 = 1.0, w = 5.0$) are shown for $n = 4$.

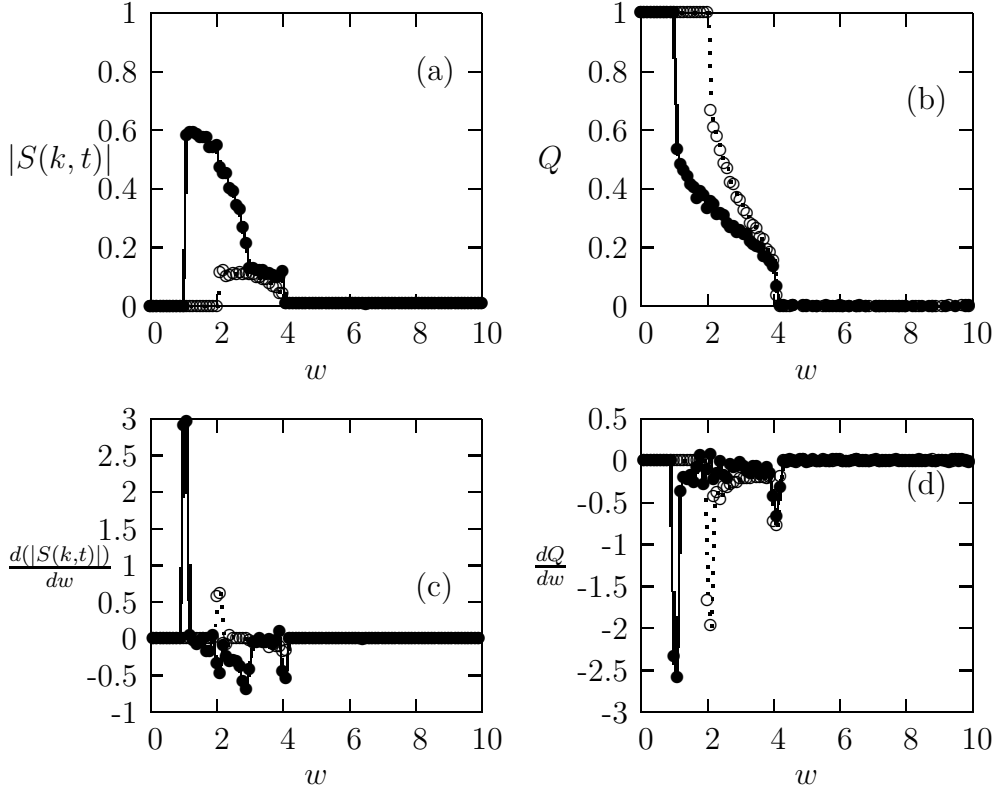


Fig-4. The $|S(k, t)|$, Q , $\frac{d(|S(k, t)|)}{dw}$ and $\frac{dQ}{dw}$ are plotted against w for bimodal distribution of quenched random field for two different values of h_0 and 4-loop of standing magnetic field wave. Different symbols represent different values of h_0 . (\bullet) represents $h_0 = 3.0$ and (\circ) represents $h_0 = 2.0$. Solid and dotted lines are just connecting the data points.

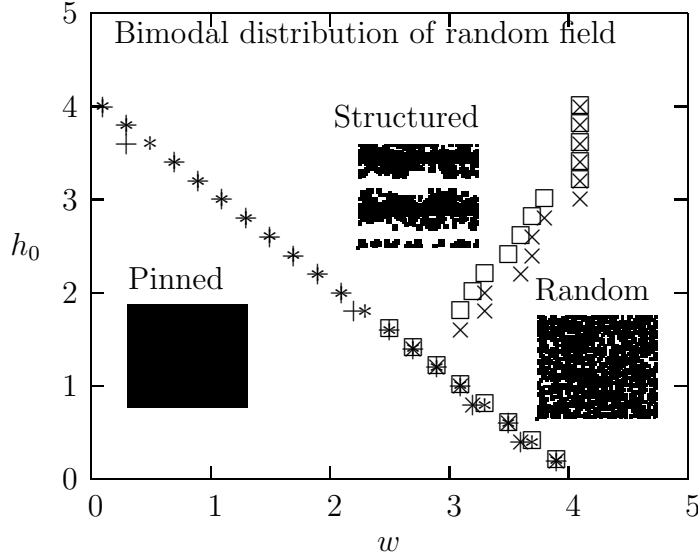


Fig-5. The phase diagram for bimodal distribution of quenched random field. The boundaries of pinned-structured (+) phase and the structured-random (\times) phase are shown for $n = 2$. The boundaries of pinned-structured (*) phases and the structured-random (\square) phases are also shown for $n = 4$. The typical spin configurations (for 60×60 lattice) are shown in the insets for three different phases. The pinned phase ($h_0 = 1.0, w = 1.0$), the structured phase ($h_0 = 2.4, w = 2.0$) and the random phase ($h_0 = 1.0, w = 4.0$) are shown for $n = 4$.

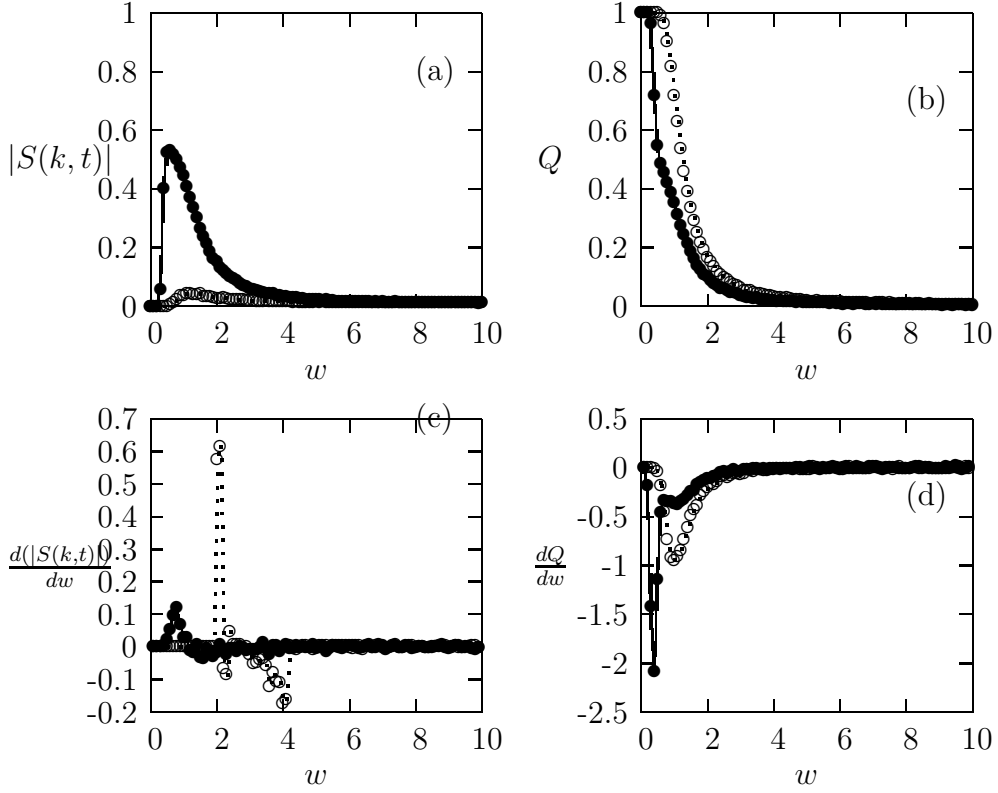


Fig-6. The $|S(k, t)|$, Q , $\frac{d(|S(k, t)|)}{dw}$ and $\frac{dQ}{dw}$ are plotted against w for Gaussian distribution of quenched random field for two different values of h_0 and 4-loop of standing magnetic field wave. Different symbols represent different values of h_0 . (\bullet) represents $h_0 = 2.2$ and (\circ) represents $h_0 = 1.0$. Solid and dotted lines are just connecting the data points.

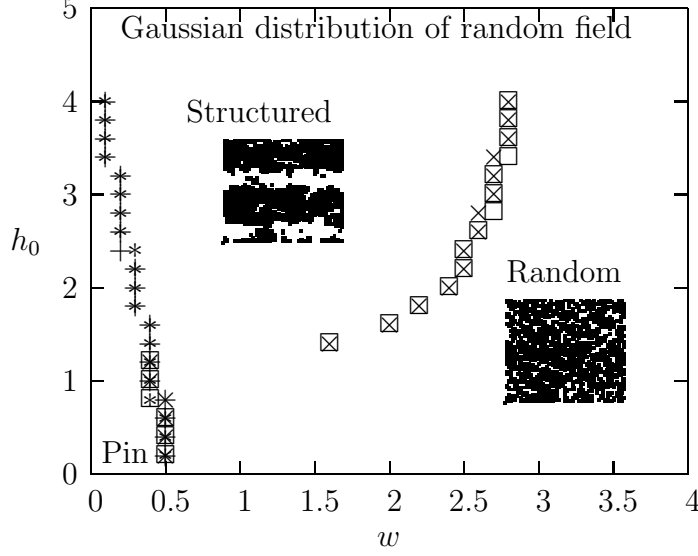


Fig-7. The phase diagram for Gaussian distribution of quenched random field. The boundaries of pinned-structured (+) phase and the structured-random (x) phase are shown for $n = 2$. The boundaries of pinned-structured (*) phases and the structured-random (□) phases are also shown for $n = 4$. The typical spin configurations (for 60×60 lattice) are shown in the insets for two different phases. The structured phase ($h_0 = 2.0$, $w = 1.0$) and the random phase ($h_0 = 1.0$, $w = 3.0$) are shown for $n = 4$. The configuration of pinned phase is similar to that for other two cases (uniform and bimodal) and could not be shown here due to the limitation of the region of space in pinned phase.